Atmos. Chem. Phys. Discuss., https://doi.org/10.5194/acp-2019-141
Manuscript under review for journal Atmos. Chem. Phys.
Discussion started: 26 February 2019

Atmospheric Chemistry and Physics Discussions
Open Access

Mixing layer transport flux of particulate matter in Beijing, China

Yusi Liu[1], Guiqian Tang[2,3], Libo Zhou[2], Bo Hu[2], Baoxian Liu[4,5], Yunting Li[4,5], Shu Liu[6], Yuesi Wang[2,3,7]

[1] State Key Laboratory of Severe Weather & Key Laboratory for Atmospheric Chemistry of China Meteorology Administration, Chinese Academy of Meteorological Sciences, Beijing 100081, China

[2] State Key Laboratory of Atmospheric Boundary Layer Physics and Atmospheric Chemistry, Institute of Atmospheric Physics, Chinese Academy of Sciences, Beijing 100029, China

[3] Center for Excellence in Urban Atmospheric Environment, Institute of Urban Environment, Chinese Academy of Sciences, Xiamen 361021, China

[4] Beijing Municipal Environmental Monitoring Centre, Beijing 100048, China

[5] Beijing Key Laboratory of Airborne Particulate Matter Monitoring Technology, Beijing 100048, China

[6] Liaoning Provincial Environmental Monitoring & Experiment Center, Shenyang 110031, China

[7] University of Chinese Academy of Sciences, Beijing 100049, China

Correspondence: Guiqian Tang (tgq@dq.cern.ac.cn)

Atmos. Chem. Phys. Discuss., https://doi.org/10.5194/acp-2019-141
Manuscript under review for journal Atmos. Chem. Phys.
Discussion started: 26 February 2019

Abstract

Quantifying the transport flux of atmospheric pollutants plays an important role in understanding the causes of atmospheric pollution and in making decisions regarding the prevention and control of atmospheric pollution. In this study, the mixing layer height and wind profile of the mixing layer were measured by ceilometer and doppler wind radar, respectively. The variation characteristics of atmospheric transport capacity (TC) were analyzed using these two datasets. The research showed that the TC appears to be strongest in spring (3940 ± 2110 $m^2\ s^{-1}$) and weakens in summer (2953 ± 1322 $m^2\ s^{-1}$), autumn (2580 ± 1601 $m^2\ s^{-1}$) and winter (2913 ± 3323 $m^2\ s^{-1}$). Combined with the near-surface fine particle concentration data, the TC influence on the $PM_{2.5}$ concentration was studied, and there is a strong inverse correlation between the $PM_{2.5}$ and TC in spring, autumn and winter (R = -0.66, -0.65 and -0.80, respectively) and a weak positive correlation in summer (R = 0.33). By calculating the transport flux of fine particles (TF), the TF in Beijing was found to be the highest in spring at 226 ± 294 mg $m^{-1}s^{-1}$ and lower in the other three seasons at approximately 140 mg $m^{-1}s^{-1}$. Transport occurs between 14:00 and 18:00 LT. Except for during spring, the TF was large in the pollution transition period (summer: 328 ± 280 mg $m^{-1}s^{-1}$, autumn: 280 ± 336 mg $m^{-1}s^{-1}$ and winter: 240 ± 297 mg $m^{-1}s^{-1}$) and decreased during the heavy pollution period (summer: 295 ± 215 mg $m^{-1}s^{-1}$, autumn: 243 ± 238 mg $m^{-1}s^{-1}$ and winter: 212 ± 209 mg $m^{-1}s^{-1}$). Our results indicate that the transportation influence in southern regions should receive more focus in the transition period of pollution, while local emissions should receive more focus in the heavy pollution period.

1. Introduction

With the rapid development of the economy and industry, as well as the unique local topography, Beijing has become one of the cities in the world that is most seriously affected by air pollution. As early as before the 2008 Olympic Games, to fulfill the promise of "Green Olympics", Beijing's industries were relocated to other provinces and cities. After the Olympic Games, with the promulgation of the "Action Plan for Prevention and Control of Air Pollution", Beijing implemented a series of measures to reduce pollutants, such as raising the emission standards of motor vehicles and fuel standards for vehicles, changing coal to natural gas, coal to electricity and so on. These measures have gradually improved the Beijing's air quality, with the concentration of fine particulate matter decreasing from 90 μg m^{-3} in 2013 to 58 μg m^{-3} in 2017 (http://www.cnemc.cn/).

Although Beijing's government has been dedicated in recent years to taking measures that could ensure a steady decrease in poor air quality, there is still great pressure to ensure the continuous decline in particulate matter concentration. Beijing is in the north of the North China Plain, the south side and the west side are the Yanshan Mountains and the Taihang Mountains, respectively. Affected by the mountains to the northwest, there are more subsiding airflows, a lower mixing layer height and an extremely limited atmospheric diffusion capacity. In addition, pollutants tend to accumulate in front of the mountains due to the influence of southerly winds and mountain obstruction. In central and northern China, the increase in $PM_{2.5}$ during winter is closely related to adverse atmospheric transport conditions (Wang et al. 2016). Therefore, in addition to primary emissions and secondary formation, weak atmospheric transport capacity (TC) is an important factor leading to the frequent occurrence of serious air pollution in Beijing.

In recent decades, mixing layer height (MLH) and wind speed (WS) are two major factors that lead

Atmos. Chem. Phys. Discuss., https://doi.org/10.5194/acp-2019-141
Manuscript under review for journal Atmos. Chem. Phys.
Discussion started: 26 February 2019

Atmospheric Chemistry and Physics
Discussions

to the annual increase in aerosol concentration and haze days during winter in China (Yang et al. 2016). Additionally, low MLH and low WS are important characteristics of weak TC (Song et al. 2014; Tang et al. 2015; Huang et al. 2018; Liu et al. 2018). The change in MLH represents the vertical TC of pollutants, and the change in WS represents the horizontal TC of pollutants. To characterize the TC, the ventilation coefficient (VC) is usually used to evaluate the vertical and horizontal transport capacity of the atmosphere (Nair et al. 2007; Tang et al. 2015; Zhu et al. 2018). Thus, it is a good choice to use VC to evaluate the relationship between TC and air pollution in Beijing. Although previous studies have analyzed the relationship between MLH and pollutants (Schäfer et al. 2006; Geiß et al. 2017; Su et al. 2018; Miao and Liu 2019), studies on the effects of VC on particle concentration are extremely rare.

In addition, with the reduction in local emission sources, the contribution of regional transport becomes particularly important. There are three main transport routes affecting Beijing: the northwest path, the southwest path and the southeast path (Chang et al. 2018; Li et al. 2018; Zhang et al. 2018). The occurrence of heavy pollution in Beijing is closely related to the transportation of pollutants in southern regions, mainly in southern Hebei, northern Henan and western Shandong, while the high-speed northwest air mass is conducive to the removal of pollutants in Beijing (Zhang et al. 2017; Li et al. 2018; Zhang et al. 2018; Ouyang et al. 2019). In recent years, the contribution of regional transport to Beijing has been increasing annually, with a trend of 1.2% year^{-1}, which reached 31-73% in summer and 27-59% in winter (Wang et al. 2015; Chang et al. 2018; Cheng et al. 2018). High $PM_{2.5}$ concentrations are usually accompanied by high transport flux within a day in Beijing (Tang et al. 2015; Zhu et al. 2016). As pollution worsens, the contribution of the surrounding areas to the $PM_{2.5}$ in Beijing has risen from 52% to 65% in a month on average (Zhao et al. 2018). However, during heavy pollution, the transport flux decreased in Beijing (Tang et al. 2015; Zhu et al. 2016; Chang et al. 2018). Although many studies on regional transport have been carried out, most observational studies cannot easily quantify transport flux due to the lack of wind profile data. Therefore, transport flux can only be obtained by models. When the model lacks verification data, the reliability of the model will decrease. Thus, it is imperative to quantify the transport flux through observations.

To solve the above two problems, we conducted 2 years of continuous observations on MLH and wind profiles in the Beijing mixing layer and analyzed the mixing layer TC of pollutants and their relationship with particulate matter. Then, combined with the concentration of particulate matter, we analyzed fine particulate matter transport flux in the mixing layer (TF). Finally, using the $PM_{2.5}$ concentration as an indicator to classify the air pollution degree, we analyzed the TF in Beijing during the transitional and heavily polluted period and illuminated the main controlling factors.

2. Methods

2.1 Observational station

To understand the TC characteristics in Beijing, two years of observations were conducted in Beijing (2016.1.1-2017.12.31). The observational site (BJT) is in the Institute of Atmospheric Physics of the Chinese Academy of Sciences, located west of the Jiande Bridge in the Haidian District, Beijing (39.98° N, 116.38° W). The north and south sides of the station are the north third and north fourth ring roads respectively, and the eastern side is Beijing-Tibet expressway. The altitude (a.s.l.) is about

60 m. There is no obvious emission source around the observational site except the highway.

2.2 Observations of MLH and wind profiles

To analyze TC, MLH was observed by a single-lens ceilometer (CL51, Vaisala, Finland), and the wind profile in the mixing layer was simultaneously observed by doppler wind radar (Windcube 100s, Leosphere, France). A single-lens ceilometer measures the attenuated backscatter coefficient profile of atmospheric aerosols by pulsed diode laser lidar technology (910 nm waveband) within a 7.7 km range, and determine the MLH through the position of abrupt changes in the backscattering coefficient profile. In the actual measurement, the measurement interval was 16 s and the measurement resolution was 10 m. More detail descriptions are presented in the published literature (Tang et al. 2016; Zhu et al. 2016). In this study, the gradient method (Steyn et al. 1999) is used to determine the MLH; that is, the top of the mixing layer was determined by the maximum negative gradient value (-dβ/dx) in the profile of the atmosphere backscattering coefficient. Moreover, to eliminate the interference of aerosol layer structure and the detection noise to data, the MLH was calculated by the improved gradient method after averaging the profile data (Münkel et al. 2007; Tang et al. 2015).

Doppler wind radar uses the remote sensor method of laser detection and ranging technology and measures the doppler frequency shift generated by the laser through the backscatter echo signal of particles in the air. Windcube 100s can provide 3D wind field data within a 3 km range from the system, including u, v and w vectors. In the actual measurement, starting from 100 m, the spatial resolution is 50 m, the WS accuracy is < 0.5 m s^{-1}, and the radial WS range is -30 m s^{-1}—30 m s^{-1}.

2.3 Other data

During the observations, the hourly $PM_{2.5}$ and ozone surface concentrations of the Beijing Olympic Sports Center (39.99° N, 116.40° W) were obtained from the Ministry of Environmental Protection of China (http://www.zhb.gov.cn/).

2.4 Analytical method

VC (m^2 s^{-1}) was obtained by combining MLH (m) and wind speed in the mixing layer (WS_{ML}, m s^{-1}), which can be used to characterize TC. A higher VC indicates a stronger TC, which is conducive to the transport and diffusion of heavy air pollution. The VC calculation method is as follows:

$$VC = MLH \times WS_{ML}, \tag{1}$$

$$WS_{ML} = \frac{1}{n}\sum_{i=1}^{n} WS_i, \tag{2}$$

$$WS = \sqrt{\overline{u}^2 + \overline{v}^2}, \tag{3}$$

where WS_{ML} is the average WS within the mixing layer, calculated by Eq. (2); WS_i is the WS observed at all heights, calculated by the mean value of u and v in the wind profile according to Eq. (3); and n is the number of measurement layers in the mixing layer (Nair et al. 2007).

TF (mg $m^{-1}s^{-1}$) is determined by TC and the $PM_{2.5}$ concentration in the area under analysis. The calculation method for a certain height is shown in Eq. (4):

$$TF_{u_1} = u_1 \times C_{PM_{2.5}} \times MLH \tag{4}$$

It is extremely difficult to observe the $PM_{2.5}$ concentration in the mixing layer by height, but previous observations have shown that the backscattering coefficient profile in the mixing layer is relatively uniform (Tang et al. 2015). Assuming that the particle concentration in the mixing layer is uniform, the TFs are calculated as follows:

$$TF_u = \frac{1}{n}\sum_{i=1}^{n} u_i \times C_{PM_{2.5}} \times MLH$$

$$TF_v = \frac{1}{n}\sum_{i=1}^{n} v_i \times C_{PM_{2.5}} \times MLH \qquad (5)$$

Through the above method, radial and zonal transport fluxes can be obtained, and vector synthesis in two directions can be conducted to obtain the main transport direction to find the transport source area.

3. Results and discussions

3.1 Mixing layer transport capacity (TC)

3.1.1 Seasonal variation

To understand the variations of TC, we carried out continuously measured MLH and wind profiles within the mixing layer over a 2-year period (2016.1.1-2017.12.31). The availability was verified after MLH elimination by Tang et al. (Tang et al. 2016). After the exclusion of the data of MLH under rainy, sandstorm and windy conditions, data availability was 95% over the 2-year period, higher than that of previous studies (Tang et al. 2016; Mues et al. 2017). The availability was lowest in February at 86% and highest in July at 99%.

The seasonal variation in MLH was higher in spring (781 ± 229 m) and summer (767 ± 219 m) and lower in autumn (612 ± 166 m) and winter (584 ± 221 m) (Fig. 1). However, WS_{ML} was quite different from MLH in terms of seasonal variation, with the largest value at 4.6 ± 1.6 m s^{-1} in spring, followed by winter (4.1 ± 2.7 m s^{-1}) and autumn (3.7 ± 1.6 m s^{-1}), and the smallest value at 3.6 ± 1.1 m s^{-1} in summer. VC was calculated by the MLH and wind profile, and the seasonal variation in TC over 2 years was analyzed (Fig. 1). The results demonstrate that the TC was strongest in spring, as the VC reached as high as 3940 ± 2110 m^2 s^{-1}. The TC differences among summer, winter and autumn were small when the VC values were 2953 ± 1322 m^2 s^{-1}, 2913 ± 3323 m^2 s^{-1} and 2580 ± 1601 m^2 s^{-1}, respectively. A monthly analysis shows that the TC was the strongest in May, the VC was as high as 5161 ± 2085 m^2 s^{-1}, the TC was the worst in December, and the VC was only 1690 ± 1072 m^2 s^{-1}. The VC value in May was 3.1 times higher than that in December. The seasonal variation in the $PM_{2.5}$ concentration was the highest in winter (80 ± 87 μg m^{-3}), followed by autumn (68 ± 54 μg m^{-3}) and spring (67 ± 60 μg m^{-3}), and the seasonal variation was the lowest in summer (51 ± 29 μg m^{-3}). The lowest monthly average $PM_{2.5}$ concentration was 42 ± 26 μg m^{-3} in August. The highest monthly average was in January at 94 ± 100 μg m^{-3}, 2.2 times higher than that in August (Fig. 1). Thus, the vertical and horizontal diffusion capacities are strong in spring and weak in autumn and winter. In summer, the vertical diffusion capacity is strong, while the horizontal diffusion capacity is weak. Overall, high $PM_{2.5}$ concentrations are associated with poor TC.

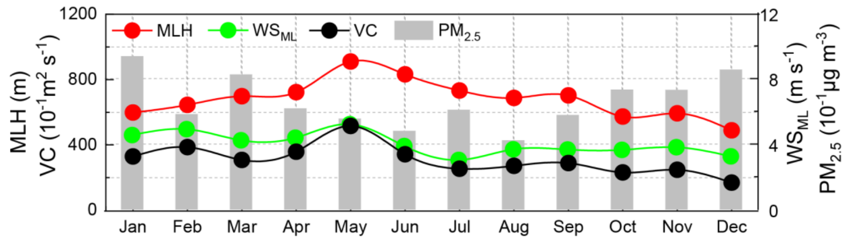

Fig. 1. Monthly variations in MLH, WS_{ML}, VC and $PM_{2.5}$ in Beijing.

3.1.2 Diurnal variation

Moreover, the diurnal variations in meteorological factors during different seasons were analyzed to reveal the diurnal evolution characteristics of atmospheric TC. The peak and trough values of MLH and VC appeared simultaneously at approximately 15:30 LT and 05:30 LT, respectively. Generally, the daily variation in MLH is characterized by a low value at night, which increases rapidly after sunrise and reaches the maximum value in the afternoon (Fig. 2a). The daily maximum value of MLH is seasonal, where it is higher in spring and summer and lower in autumn and winter. The daily minimum value of MLH generally occurs when the mixing layer is stable and is closely related to WS. The diurnal variation in WS_{ML} is stable, with a peak at approximately 19:30 LT and a trough at approximately 10:00 LT, which is 4 h later than the peak valley of MLH (Fig. 2b). The diurnal variation in VC is similar to MLH, showing that the TC is strong before sunset, gradually weakens after sunset and remains stable at night. The TC in spring was significantly stronger than that during other seasons, and the maximum daily value reached 8678 $m^2 s^{-1}$ (Fig. 2c). In addition to spring, the daily maximum values of VC in summer, autumn and winter were close at approximately 5000 $m^2 s^{-1}$ (Fig. 2c). The TC growth rate in spring was significantly higher than that in other seasons, reaching a maximum at approximately 09:00 LT. Late in autumn, the TC growth rate peaked at approximately 10:00 LT. Summer and winter peaked at approximately 11:00 LT. Throughout the year, VC began to increase during winter at the latest, at approximately 09:00 LT, indicating that the weaker TC remained for a longer period during winter. TC was weakened most rapidly in spring; however, the TC was still higher than the VC of other seasons after declining. In addition to spring, the TC in autumn and winter weakened the most rapidly and the slowest in summer. In general, vertical and horizontal diffusion is very strong in the spring during both day and night. In winter, vertical diffusion is weak during the day, and horizontal transportation during the night is the main transportation. In summer, vertical diffusion during the day is dominant.

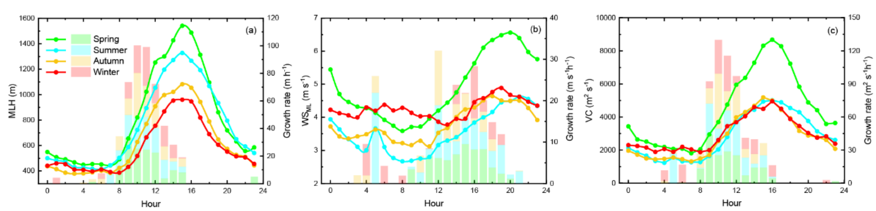

Fig. 2. Diurnal variations and growth rates of MLH (a), WS_{ML} (b) and VC (c) in spring, summer, autumn and winter in Beijing. Diurnal variations are represented by lines and scatters. Growth rates are represented by columns, and only positive values are shown in the figure.

Atmos. Chem. Phys. Discuss., https://doi.org/10.5194/acp-2019-141
Manuscript under review for journal Atmos. Chem. Phys.
Discussion started: 26 February 2019

3.1.3 Frequency distribution

Although there is little difference in TC between summer, autumn and winter, there is serious pollution in autumn and winter. To analyze this problem, the VC frequency distribution was studied. The results show that VC had a high frequency in the range of 1000-4000 $m^2 s^{-1}$ from 2016 to 2017, but the frequency distribution was different in different seasons (Fig. 3). The VC showed a strong TC in spring, mainly in the range of 2000-5000 $m^2 s^{-1}$, with the highest frequency (24%) in the range of 2000-3000 $m^2 s^{-1}$. In summer, the high frequency of VC occurred in the range of 1000-4000 $m^2 s^{-1}$, which was slightly lower than that in spring, and the highest frequency (27%) occurred in the range of 3000-4000 $m^2 s^{-1}$. Additionally, the VC high frequency appeared in a lower range in autumn and winter. The VC occurred at a high frequency of 1000-3000 $m^2 s^{-1}$ in autumn, and the highest frequency occurred within the range of 2000-3000 $m^2 s^{-1}$, accounting for 33%. In winter, VC appeared more frequently in the range of 0-2000 $m^2 s^{-1}$ and was the highest in the range of 1000-2000 $m^2 s^{-1}$, which was 28%. However, the VC frequency of 0-1000 $m^2 s^{-1}$ in winter was significantly higher than that of the other seasons, up to 22%, which was 7 times higher than that of spring, 5 times higher than that of summer and 2 times higher than that of autumn. According to the seasonal variation in $PM_{2.5}$ concentration, heavy pollution in autumn and winter is related to the high frequency of poor TC.

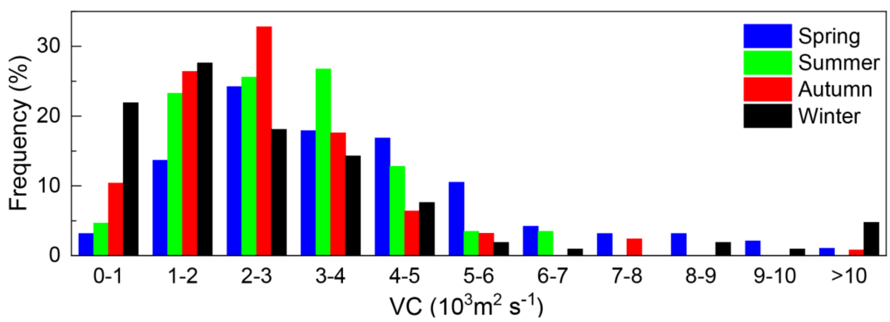

Fig. 3. Frequency distribution of the daily VC from January 2016 to December 2017 in Beijing.

3.2 Response of particulate matter to TC

Studies have found that air pollution worsens when TC weakens (Tang et al. 2015; Liu et al. 2018; Sun et al. 2018). To further understand the response of fine particles to TC in different seasons, the correlations between meteorological factors and $PM_{2.5}$ concentration were analyzed (Fig. 4). From 2016 to 2017, the annual average $PM_{2.5}$ concentration was 66 ± 62 μg m^{-3}, the maximum concentration was 898 μg m^{-3}, and the minimum concentration was only 1 μg m^{-3}, which showed high concentrations in autumn and winter. As shown in Fig. 4, $PM_{2.5}$ concentrations increased exponentially with decreases in MLH, WS_{ML} and VC, indicating that the concentration of fine particles was highly sensitive to these meteorological factors. When MLH, WS_{ML} and VC were lower than 400 m, 2.5 m s^{-1} and 1500 $m^2 s^{-1}$, respectively, the air pollution declines sharply. VC had a better correlation with the $PM_{2.5}$ concentration than MLH and WS_{ML}, indicating that VC can better characterize pollution dissipation. The $PM_{2.5}$ concentration in winter had a better response to TC than the other seasons, with the correlation coefficient with VC reaching -0.80, followed by spring

Atmos. Chem. Phys. Discuss., https://doi.org/10.5194/acp-2019-141
Manuscript under review for journal Atmos. Chem. Phys.
Discussion started: 26 February 2019

Atmospheric Chemistry and Physics Discussions
Open Access

and autumn, with correlation coefficients of -0.66 and -0.65, respectively (Fig. 4). The correlation in spring and autumn may decrease due to dust. In summer, $PM_{2.5}$ had a poor relationship with WS_{ML} and even had weak positive correlations with MLH (R = 0.42) and VC (R = 0.33). A high ozone concentration existed in the high MLH (Fig. 4), which will promote the transformation of gaseous precursors to secondary particles. Therefore, the weak positive correlation in summer was related to a strong photochemical reaction.

Thus, MLH, WS_{ML} and VC can be used as indicator factors for the formation of air pollution, but the particle concentration responds best to VC. Additionally, the response of particle concentration to VC showed obvious seasonal differences, with the best in winter, followed by autumn and spring, and a weak positive correlation in summer.

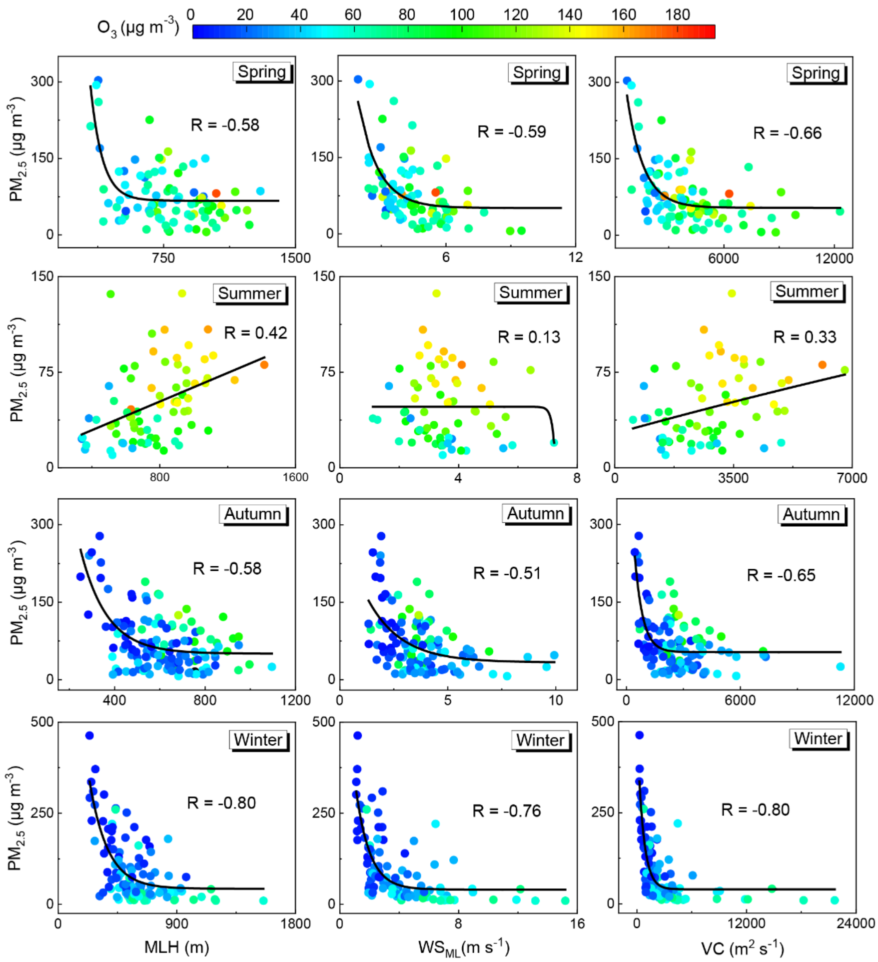

Fig. 4. Correlations among MLH, WS_{ABL} and VC and $PM_{2.5}$ under different ozone levels in Beijing.

Atmos. Chem. Phys. Discuss., https://doi.org/10.5194/acp-2019-141
Manuscript under review for journal Atmos. Chem. Phys.
Discussion started: 26 February 2019

3.3 Mixing layer transport flux of particulate matter

To quantify the transport of pollutants in Beijing, the Beijing TF was analyzed, and the transport direction of fine particles was characterized by the wind direction in the mixing layer. As shown in Fig. 5, the TF in spring was the largest, reaching 226 ± 294 mg m^{-1}s^{-1}, and there was no significant difference in summer, autumn or winter, when the TF values were 147 ± 182 mg m^{-1}s^{-1}, 143 ± 194 mg m^{-1}s^{-1} and 134 ± 179 mg m^{-1}s^{-1}, respectively. The northwesterly and westerly directions were the main transport sources of the cold period in Beijing. With temperature warming, the transport direction gradually increased from west to south, mainly as a southwesterly in spring and southerly in summer. The monthly average maximum value of TF occurred in May, as high as 269 ± 328 mg m^{-1}s^{-1} and mainly originated from the southwest direction, which was accompanied by a strong wind. The minimum value appeared in August, as low as 106 ± 145 mg m^{-1}s^{-1}, which was mainly transported from western regions, with low WS values. The TF in May was 2.5 times higher than that in August (Fig. 5). Therefore, the change in transport direction leads to an obvious seasonal variation in TF. Overall, the regional transport contributes the most to the particulate matter concentration in spring, which is mainly related to increased dust activities; regional transport has the least contribution in winter, which indicates that more focus should be given to local emission source control; in summer and autumn, the southwest airflow transportation influence on Beijing should receive more focus.

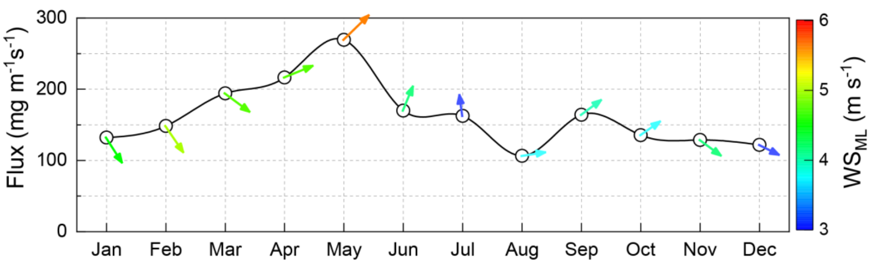

Fig. 5. Seasonal variations in the mixing layer transport flux of PM and transportation directions.

To understand the regional transport influence on the Beijing area, the diurnal variation characteristics of TF were analyzed during different seasons in Beijing. The daily minimum value of TF appeared at approximately 07:00 LT and was accompanied by a northerly wind. As the wind direction gradually turned south, the daily minimum value of TF continued to rise until the daily maximum value appeared at approximately 16:00 LT (Fig. 6). Transportation mainly occurred between 14:00 and 18:00 LT, which was consistent with the results of a previous study (Ge et al. 2018). In spring, the WS was higher, so the peak TF duration was shorter, at approximately 2 h. The maximum daily value was 494 mg m^{-1}s^{-1}, and the minimum was 87 mg m^{-1}s^{-1} in spring. Therefore, the diurnal variation in TF during spring showed the characteristics of a rapid rise and rapid decline. The peak duration was approximately 4 h for a long time in summer and autumn, where the daily maximum values were 259 mg m^{-1}s^{-1} and 240 mg m^{-1}s^{-1}, and the minimum values were 53 mg m^{-1}s^{-1} and 66 mg m^{-1}s^{-1}, respectively. The diurnal variation in TF during summer and autumn showed the characteristics of a slow rise and slow decline. Specifically, the daily variation had a strong fluctuation in winter, which peaked at only 16:00 LT (215 mg m^{-1}s^{-1}), then dropped sharply to 193 mg m^{-1}s^{-1}, plateaued from 17:00 to 22:00 LT for approximately 5 h, maintained at approximately 176 mg m^{-1}s^{-1}, and then quickly dropped to 78 mg m^{-1}s^{-1}

Atmos. Chem. Phys. Discuss., https://doi.org/10.5194/acp-2019-141
Manuscript under review for journal Atmos. Chem. Phys.
Discussion started: 26 February 2019

The TF variation rules can be summarized as a high TF corresponds to a southerly wind and a low TF corresponds to a northerly wind. When the wind direction in the mixing layer changed from north to south, the wind gradually increased from the daily minimum to the daily maximum. The TF increased by 6 times in spring, 5 times in summer, 4 times in autumn and 3 times in winter. The current pattern is because areas south of Beijing are heavily polluted and southerly winds help transport pollutants into the city, leading to high transport flux in spring, summer and autumn afternoons (Fig. 6). The results further confirm the conclusion that the northwest wind in Beijing is a clean wind (Wang et al. 2015; Zhang et al. 2018). Thus, the north wind is conducive to the outward transport of pollutants from Beijing, which helps to alleviate pollution. As a result, there was no high TF in winter when the westerly wind and northerly wind prevailed. This finding also proves the important influence of local emissions on heavy pollution occurrence during winter in Beijing. In summary, there are 4 main transport routes that affect Beijing, including the northwest path, southwest path, west path and south path. The TF in winter is low, local emissions play an important role, and we must pay attention to local pollutant emission control.

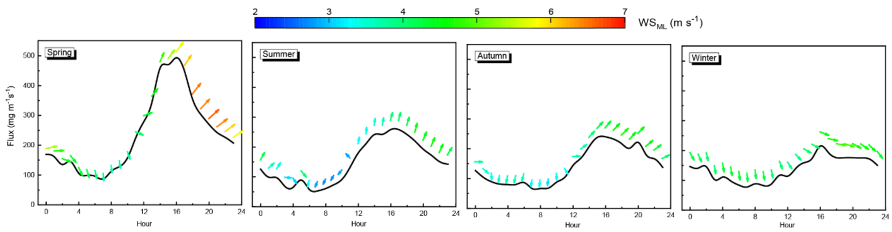

Fig. 6. Diurnal variations in the mixing layer transport flux of PM and transportation directions during different seasons in Beijing.

3.4 TF under different degrees of air pollution

Previous studies have demonstrated that transportation occurs only at the transition period of pollution, and transportation is weak at the peak of pollution (Tang et al. 2015; Zhu et al. 2016). To quantify the transport impact of different pollution levels, the $PM_{2.5}$ concentration was divided into five levels according to the "Technical Regulation on Ambient Air Quality Index (on trial)" (HJ 633-2012): $PM_{2.5} \leq 35$ μg m^{-3} (clear days), $35 < PM_{2.5} \leq 75$ μg m^{-3} (slight haze), $75 < PM_{2.5} \leq 115$ μg m^{-3} (light haze), $115 < PM_{2.5} \leq 150$ μg m^{-3} (medium haze) and $PM_{2.5} > 150$ μg m^{-3} (heavy haze). With pollution aggravation, the TF in Beijing increased by varying degrees during different seasons, and the transportation direction gradually shifted from northwest to south (except during winter) (Fig. 7). In particular, the TF continued to increase only in spring, from 93 ± 124 mg m^{-1}s^{-1} on clear days to 382 ± 438 mg m^{-1}s^{-1} on heavily polluted days, which may be caused by more dust during spring. With the except of during spring, with pollution deterioration, the TF showed an increasing trend at the initial stage of pollution and decreasing trend during the heavy pollution period. From medium haze to heavy haze, the TF decreased from 328 ± 280 mg m^{-1}s^{-1} to 295 ± 215 mg m^{-1}s^{-1}in summer, from 280 ± 336 mg m^{-1}s^{-1} to 243 ± 238 mg m^{-1}s^{-1} in autumn, and from 240 ± 297 mg m^{-1}s^{-1} to 212 ± 209 mg m^{-1}s^{-1} in winter. These results indicate that although the region south of Beijing is the main transport source during summer and autumn in Beijing, this contribution is significantly reduced during the severe pollution period. In winter, with pollution aggravation, the transportation direction changed from northwest to southwest and finally to the north. In contrast to

Atmos. Chem. Phys. Discuss., https://doi.org/10.5194/acp-2019-141
Manuscript under review for journal Atmos. Chem. Phys.
Discussion started: 26 February 2019

other seasons, the north wind with a low WS was the main wind during heavy pollution in winter, indicating that regional transport contributed less to heavy pollution during winter in Beijing. In general, the transport of pollutants from the southwest is the main controlling factor for pollution occurrence during spring in Beijing. In other seasons, regional transport plays an important role in the initial period of pollution, while local emissions during the period of heavy pollution are the main controlling factor.

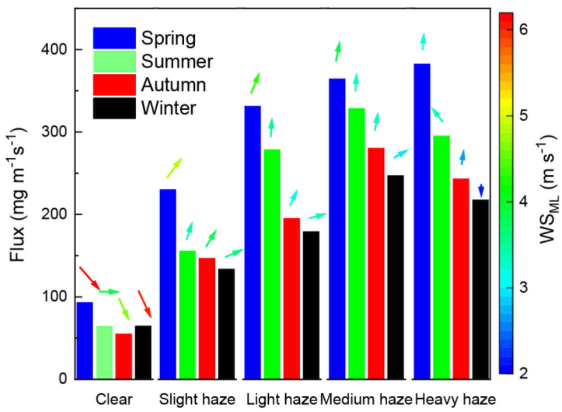

Fig. 7. The mixing layer transport flux levels of PM and transportation directions under different degrees of pollution.

4. Conclusions

To understand the characteristics of fine particulate matter transport flux in Beijing, the height of the atmospheric mixing layer and wind profile within the mixing layer in Beijing were observed for a 2-year period. The main conclusions are as follows:

(1) By analyzing the variation characteristics of VC, the TC in Beijing is strongest in spring and weaker in summer, autumn and winter. In spring, vertical and horizontal diffusion capacities are strong; in autumn and winter, vertical and horizontal diffusion capacities are weak; in summer, vertical diffusion capacity is strong and horizontal diffusion capacity is weak. The diurnal variation in VC is consistent with MLH, which shows that the TC is strongest before sunset, gradually weakens after sunset and remains stable at night. In spring, vertical and horizontal diffusion are very strong during both day and night. In winter, vertical diffusion is weak during the day, and horizontal transportation during the night is the main means of transportation. In summer, vertical diffusion during the day is dominant. Although there is little difference in diffusivity between summer, autumn and winter, poor TC occurs more frequently in autumn and winter.

(2) $PM_{2.5}$ concentrations during different seasons have different responses to MLH, WS_{ML} and VC. During the three dry seasons of winter, spring and autumn, the concentration of pollutants has a good relationship with VC, indicating that the main dissipation method of pollutants is diffusion. In summer, there is a weak positive correlation between pollutant concentration and VC, which is related to strong photochemical reactions.

(3) TF is largest in spring and smaller in summer, autumn and winter in Beijing. The high TF mainly comes from southward transport, while the low TF is accompanied by northwest transport. Using

the $PM_{2.5}$ concentration as a classified index of atmospheric pollution, the results show that the regional transport of pollutants from the southwest is the main controlling factor of pollution during spring in Beijing, while during the other seasons, the regional transport from the southern area plays an important role in the initial period of pollution, and local emissions are the main controlling factors in the heavy pollution period, especially in winter.

In this study, the response of particulate matter to meteorological conditions in the mixing layer was studied, and the difference in the seasonal response was found. The transport capacity during different seasons and the transport flux during different pollution periods were also discussed. The research results are of great significance to the early warning, prevention and control of atmospheric particulate pollution. However, due to the limitation of observational data, the near-surface particle concentration was used to replace the concentration column for discussion purposes, resulting in uncertainty in the result. In the future, this issue will be further discussed in combination with ground-based telemetry lidar.

Data availability

The data in this study are available from the corresponding author upon request (tgq@dq.cern.ac.cn).

Author contribution

GT and YW designed the research, LZ, BH, BL and YunL conducted the measurements. YusL and GT wrote the paper. SL reviewed and commented on the paper.

Competing interests

The authors declare that they have no conflict of interest.

Acknowledgments

This work was supported by the National Key R&D Program of China (2018YFC0213201), the Young Talent Project of the Center for Excellence in Regional Atmospheric Environment CAS (CERAE201802), LAC/CMA (2017A01), the National research program for key issues in air pollution control (DQGG0101), and the National Natural Science Foundation of China (Nos. 41705113 and 41877312).

References

Chang, X., S. Wang, B. Zhao, S. Cai, and J. Hao: Assessment of inter-city transport of particulate matter in the Beijing–Tianjin–Hebei region, Atmos. Chem. Phys., 18, 4843-4858, https://doi.org/10.5194/acp-18-4843-2018, 2018.

Cheng, N., Y. Li, B. Cheng, X. Wang, F. Meng, Q. Wang, and Q. Qiu: Comparisons of two serious air pollution episodes in winter and summer in Beijing, J. Environ. Sci-China., 69, 141-154, https://doi.org/10.1016/j.jes.2017.10.002, 2018.

Ge, B., Z. Wang, W. Lin, X. Xu, J. Li, D. Ji, and Z. Ma: Air pollution over the North China Plain and its

Atmos. Chem. Phys. Discuss., https://doi.org/10.5194/acp-2019-141
Manuscript under review for journal Atmos. Chem. Phys.
Discussion started: 26 February 2019

Atmospheric Chemistry and Physics
Open Access
Discussions

implication of regional transport: A new sight from the observed evidences, Environ. Pollut., 234, 29-38, https://doi.org/10.1016/j.envpol.2017.10.084, 2018.

Geiß, A., M. Wiegner, B. Bonn, K. Schäfer, R. Forkel, E. von Schneidemesser, C. Münkel, K.L. Chan, and R. Nothard: Mixing layer height as an indicator for urban air quality?, Atmos. Meas. Tech., 10, 2969-2988, https://doi.org/10.5194/amt-10-2969-2017, 2017.

Huang, Q., X. Cai, J. Wang, Y. Song, and T. Zhu: Climatological study of the boundary-layer air stagnation Index for China and its relationship with air pollution, Atmos. Chem. Phys., 18, 7573-7593, https://doi.org/10.5194/acp-18-7573-2018, 2018.

Li, H., F. Duan, Y. Ma, K. He, L. Zhu, T. Ma, S. Ye, S. Yang, T. Huang, and T. Kimoto: Case study of spring haze in Beijing: Characteristics, formation processes, secondary transition, and regional transportation, Environ. Pollut., 242, 544-554, https://doi.org/10.1016/j.envpol.2018.07.001, 2018.

Liu, L., J. Guo, Y. Miao, L. Liu, J. Li, D. Chen, J. He, and C. Cui: Elucidating the relationship between aerosol concentration and summertime boundary layer structure in central China, Environ. Pollut., 241, 646-653, https://doi.org/10.1016/j.envpol.2018.06.008, 2018.

Miao, Y., and S. Liu: Linkages between aerosol pollution and planetary boundary layer structure in China, Sci. Total. Environ, 650, 288-296, https://doi.org/10.1016/j.scitotenv.2018.09.032, 2019.

Mues, A., M. Rupakheti, C. Münkel, A. Lauer, H. Bozem, P. Hoor, T. Butler, and M.G. Lawrence: Investigation of the mixing layer height derived from ceilometer measurements in the Kathmandu Valley and implications for local air quality, Atmos. Chem. Phys., 17, 8157-8176, https://doi.org/10.5194/acp-17-8157-2017, 2017.

Münkel, C., N. Eresmaa, J. Räsänen, and A. Karppinene: Retrieval of mixing height and dust concentration with lidar ceilometer, Bound-Lay. Meteorol, 124, 117-128, https://doi.org/10.1007/s10546-006-9103-3, 2007.

Nair, V.S., K.K. Moorthy, D.P. Alappattu, P.K. Kunhikrishnan, S. George, P.R. Nair, S.S. Babu, B. Abish, S.K. Satheesh, S.N. Tripathi, K. Niranjan, B.L. Madhavan, V. Srikant, C.B.S. Dutt, K.V.S. Badarinath, and R.R. Reddy: Wintertime aerosol characteristics over the Indo-Gangetic Plain (IGP): Impacts of local boundary layer processes and long-range transport, J. Geophys. Res-Atmos., 112, D13205, https://doi.org/10.1029/2006jd008099, 2007.

Ouyang, W., Y. Xu, J. Cao, X. Gao, B. Gao, Z. Hao, and C. Lin: Rainwater characteristics and interaction with atmospheric particle matter transportation analyzed by remote sensing around Beijing, Sci. Total Environ., 651, 532-540, https://doi.org/10.1016/j.scitotenv.2018.09.120, 2019.

Schäfer, K., S. Emeis, H. Hoffmann, and C. Jahn: Influence of mixing layer height upon air pollution in urban and sub-urban areas, Meteorol. Z., 15, 647-658, https://doi.org/10.1127/0941-2948/2006/0164, 2006.

Song, L.C., G. Rong, L. Ying, and W. Guo-Fu: Analysis of China's haze days in the winter half-year and the climatic background during 1961–2012, Advances in Climate Change Research, 5, 1-6, https://doi.org/10.3724/sp.j.1248.2014.001, 2014.

Steyn, D.G., M. Baldi, and R.M. Hoff: The detection of mixed layer depth and entrainment zone thickness from lidar backscatter profiles, J. Atmos. Ocean. Technol., 16, 953-959, https://doi.org/, 1999.

Su, T., Z. Li, and R. Kahn: Relationships between the planetary boundary layer height and surface pollutants derived from lidar observations over China, Atmos. Chem. Phys., 18, 15921-15935, https://doi.org/10.5194/acp-18-15921-2018, 2018.

Sun, T., H. Che, B. Qi, Y. Wang, Y. Dong, X. Xia, H. Wang, K. Gui, Y. Zheng, H. Zhao, Q. Ma, R. Du, and X. Zhang: Aerosol optical characteristics and their vertical distributions under enhanced haze pollution events: effect of the regional transport of different aerosol types over eastern China, Atmos. Chem. Phys., 18, 2949-2971, https://doi.org/10.5194/acp-18-2949-2018, 2018.

Tang, G., J. Zhang, X. Zhu, T. Song, C. Münkel, B. Hu, K. Schäfer, Z. Liu, J. Zhang, L. Wang, J. Xin, P. Suppan, and Y. Wang: Mixing layer height and its implications for air pollution over Beijing, China, Atmos. Chem. Phys., 16, 2459-2475, https://doi.org/10.5194/acp-16-2459-2016, 2016.

Tang, G., X. Zhu, B. Hu, J. Xin, L. Wang, C. Munkel, G. Mao, and Y. Wang: Impact of emission controls on air quality in Beijing during APEC 2014: lidar ceilometer observations, Atmos. Chem. Phys., 15, 12667-12680, https://doi.org/10.5194/acp-15-12667-2015, 2015.

Wang, L., Z. Liu, Y. Sun, D. Ji, and Y. Wang: Long-range transport and regional sources of PM2.5 in Beijing based on long-term observations from 2005 to 2010, Atmos. Res., 37-48, https://doi.org/10.1016/j.atmosres.2014.12.003, 2015.

Wang, X., K. Wang, and L. Su: Contribution of Atmospheric Diffusion Conditions to the Recent Improvement in Air Quality in China, Sci. Rep-UK., 6, 36404, https://doi.org/10.1038/srep36404, 2016.

Yang, Y., H. Liao, and S. Lou: Increase in winter haze over eastern China in recent decades: Roles of variations in meteorological parameters and anthropogenic emissions, J. Geophys. Res. Atmos., 121, 13,050-013,065, https://doi.org/10.1002/2016jd025136, 2016.

Zhang, H., S. Cheng, X. Wang, S. Yao, and F. Zhu: Continuous monitoring, compositions analysis and the implication of regional transport for submicron and fine aerosols in Beijing, China, Atmos. Environ., 195, 30-45, https://doi.org/10.1016/j.atmosenv.2018.09.043, 2018.

Zhang, Y., J. Chen, H. Yang, R. Li, and Q. Yu: Seasonal variation and potential source regions of PM2.5-bound PAHs in the megacity Beijing, China: Impact of regional transport, Environ. Pollut., 231, 329-338, https://doi.org/10.1016/j.envpol.2017.08.025, 2017.

Zhao, D.F., S.H. Schmitt, M.J. Wang, I.H. Acir, R. Tillmann, Z.F. Tan, A. Novelli, H. Fuchs, I. Pullinen, R. Wegener, F. Rohrer, J. Wildt, A. Kiendler-Scharr, A. Wahner, and T.F. Mentel: Effects of NOx and SO2 on the secondary organic aerosol formation from photooxidation of alpha-pinene and limonene, Atmos. Chem. Phys., 18, 1611-1628, https://doi.org/10.5194/acp-18-1611-2018, 2018.

Zhu, X., G. Tang, J. Guo, B. Hu, T. Song, L. Wang, J. Xin, W. Gao, C. Münkel, K. Schäfer, X. Li, and Y. Wang: Mixing layer height on the North China Plain and meteorological evidence of serious air pollution in southern Hebei, Atmos. Chem. Phys., 18, 4897-4910, https://doi.org/10.5194/acp-18-4897-2018, 2018.

Zhu, X.W., G.Q. Tang, B. Hu, L.L. Wang, J.Y. Xin, J.K. Zhang, Z.R. Liu, C. Munkel, and Y.S. Wang: Regional pollution and its formation mechanism over North China Plain: A case study with ceilometer observations and model simulations, J. Geophys. Res-Atmos., 121, 14574-14588, https://doi.org/10.1002/2016jd025730, 2016.